# STRESS-DEPENDENT POROSITY AND PERMEABILITY OF A SUITE OF SAMPLES FROM SAUDI ARABIAN SANDSTONE AND LIMESTONE RESERVOIRS

M. A. Mohiuddin[*1], G. Korvin[2], A. Abdulraheem[1], M. R. Awal[1], K. Khan[1], M. S. Khan[1] & H. M. Hassan[1]

## ABSTRACT

A study has been conducted to understand the behavior of the stress-dependent porosity and permeability of fifty Saudi Arabian reservoir rock samples. Half of the samples were sandstones, the other half limestones. The range of confining pressure was 0-82 MPa. Nine simultaneous measurements of porosity and permeability were taken in this range during loading, and four measurements during unloading, to estimate the amount of hysteresis. The pressure pulse decay technique was used to measure permeability for very tight sandstone samples.

Fundamental differences in the stress-dependent porosity and permeability behavior of sandstone and limestone were observed. In general, both porosity and permeability decreased with increasing stress. The porosity-pressure curve for sandstones was convex from upward, and for limestone convex from downwards. Simple analytical expressions were found to describe the porosity-, and permeability vs. pressure dependencies.

In most of the sandstone samples the loss in porosity and permeability was regained during the downloading cycle, i.e. there was no appreciable hysteresis. This could be due to the fact that the pores were compressible and regained their original state after removing the pressure. However for limestone samples the hysteresis was appreciable because the pores were of incompressible or mixed type. Some limestone samples, which were characterized by high porosity and permeability, showed a sharp drop both in porosity and permeability at about 70 MPa confining pressure. This sharp decrease was not regained during downloading, because of a possible pore collapse.

## INTRODUCTION

Hydrocarbon reservoirs can be regarded as complex interacting systems of rock, oil, water and gas permitting the storage and flow of hydrocarbon fluids. A typical reservoir formation consists of a porous rock mass with varying amount of oil, gas and

[*] Corresponding Author; email: mamuddin@kfupm.edu.sa
[1] Center for Petroleum & Minerals, Research Institute, King Fahd University of Petroleum & Minerals, Dhahran – 31261, Saudi Arabia.
[2] Earth Sciences Department, King Fahd University of Petroleum & Minerals, Dhahran, Saudi Arabia.

formation brine occupying the pore spaces. Reservoir rocks are subjected to in-situ stresses arising from the combined effects of overburden pressures which is exerted by the weight of overlying rocks, tectonic stresses that are generated by large-scale movements in the Earth's crust, and pore pressure that is exerted by the fluids present in the rock pores. On the basis of their mode of action, these stresses can be further decomposed into two parts: external stress and internal pressure. Further, effective stress which represents the stress carried by the rigid rock skeleton, is defined as the algebraic difference between the external stress and internal pressure. Biot's constant is assumed to be one for these rocks samples. When effective stress is compressive its action attempts to bring about a reduction in the volume of the rock. The pore pressure acts to reduce the effective stress, thereby providing internal support to the rock skeleton that resists the "crushing" effect of the effective stress. As reservoirs get depleted during production the pore pressure decreases. This causes an increase in effective stress which leads to a reduction of pore volume. This reduction affects the porosity and permeability of a stress-sensitive reservoir.

As hydrocarbon reservoirs are found at greater depths, understanding stress-dependent permeability becomes essential. Under large draw-down, reduced permeability can lower the production from a stress-sensitive reservoir. Understanding of stress-dependent porosity is useful in estimating the remaining reserves of hydrocarbons in a producing stress-sensitive reservoir.

Jones (1988) presented empirical equations that fit permeability and porosity data versus confining pressure. Each of these equations has four adjustable parameters. He also presented a way to estimate the porosity and permeability at any pressure of interest between 0 – 10,000 psi by making only two measurements. This is made possible by presetting two of the four adjustable parameters.

Luffel et al. (1991) derived an empirical relationship between core permeability and porosity at reservoir stress. Porosity and permeability were measured at ambient conditions and at reservoir stress for a large number of core samples form Travis peak tight sandstone gas reservoir. It was concluded that correlations are improved when applied to specific environmental rock types.

Davies and Holditch (1998) identified the main factor controlling stress-dependent permeability as pore geometry, in particular, the size and shape of the pore throat. They suggested an indirect way of estimating permeability in-situ, with the help of wireline logs. The logs would identify the rock type and using the correlations between porosity and permeability developed for different rock types, the in-situ permeability can be estimated.

Davies and Davies (1999) considered pore geometry as a fundamental control on stress-dependent permeability in unconsolidated and consolidated sandstone reservoirs. They also stated that in unconsolidated sand reservoirs, the greatest permeability reduction with stress occurs in the sands with the highest values of porosity and permeability. In cemented sandstone reservoirs, the opposite is the case: most of the reduction in

permeability occurs in sandstones with the lowest values of porosity and permeability. This difference in the behavior between unconsolidated and consolidated reservoir sands is controlled by pore geometry. They also presented a reservoir simulation study incorporating the stress dependency of permeability, and indicated that it can have a significant effect on the performance of an individual well as well as the reservoir.

It is essential to understand the stress-dependent porosity and permeability for reliable modeling of the reservoir during production, particularly for stress-sensitive reservoirs during large drawdowns. This understanding will aid in economic and judicious recovery of hydrocarbons and in forecasting the remaining reserves at any point of production life. Most of the literature (Luffel, 1991; Davies and Holditch, 1998; Davies and Davies, 1999) are devoted to finding a relationship between porosity and permeability at in-situ conditions only. The confining pressure for the reservoir condition is evaluated as overburden pressure minus the pore pressure at the point of abandoning the reservoir. The correlation between porosity and permeability determined this way is valid only at one effective stress representative of the fag end of life of the reservoir. Consequently, the correlation is not useful to predict the porosity and permeability changes occurring during production. Moreover, it is noticed that, in the literature majority of the work is done for sandstone. Very few attempts have been made to understand the stress-dependent porosity and permeability behavior of limestone reservoirs.

In the present study, stress-dependent porosity and permeability of fifty Saudi Arabian reservoir core samples in the confining pressure range of 0-82 MPa were measured. The suite of fifty samples comprised of equal number of sandstone and limestone reservoir rocks. Fundamental differences in the stress-dependent porosity and permeability behavior of sandstone and limestone samples were observed. The differences could be due to the different types of pores present in sandstones and limestones. Simple analytical expressions were obtained to describe the porosity-, and permeability versus pressure dependencies. Correlations between the different parameters of the curve fits were also established.

## EXPERIMENTAL PROCEDURE

All measurements were performed on cylindrical shaped rock samples of 1.5 *in* diameter and 1.0 *in* length. The samples were cleaned using toluene and alcohol in Soxhlet type extractor and then dried in a vacuum oven.

### Measurement of Porosity and Permeability

The porosity and permeability of the rock samples were measured simultaneously at every step of the pressure cycle. A combined porosity and permeability measurement apparatus was assembled for this purpose (Abdulraheem et al., 1999). The porosity was measured using the Helium gas expansion method. The permeability was measured either by the steady state method or by the pressure pulse decay technique (Figure 1) for very tight samples. As mentioned earlier, the range of confining pressure was 0-82 MPa. The

pore pressure during porosity and permeability measurements is negligible compared to the externally applied hydrostatic confining pressure. Nine simultaneous measurements of porosity and permeability in this range during loading and four measurements during unloading were made. Enough time was given at every pressure step for the stress to equilibrate and the corresponding strains to fully develop. It is to be noted that only one method of measuring permeability is used for all the pressure steps during a loading and unloading cycle. Pressure pulse method is used only for a small number of sandstone samples with initial permeability less than 0.1 md at 4.12 MPa confining pressure.

The procedure and theory for measuring the porosity by gas expansion method and permeability by steady state method can be found in the standard text (Tiab and Donaldson, 1996). A brief review of determination of permeability by pressure pulse decay method is provided below.

**Pressure Pulse Decay Method**

The schematic diagram showing the experimental setup of the transient pressure pulse decay method is shown in Figure 1. The procedure can be described in the following points:

- The system consisting of the core holder and the upper and lower reservoirs is brought to a certain pressure called the system pressure.
- The upper reservoir is isolated and its pressure is increased by about 2-3% of the system pressure.
- The pressure pulse is made to flow through the rock specimen and its decay with respect to time is recorded by the data acquisition system. The pressure decay data can be used to determine the permeability of the rock specimen.

The reader is referred to Hsieh et al. (1980) for the theory of the pressure pulse decay method. For faster pulse-decay permeability measurement in tight rocks, a laboratory technique developed by Jones (1994) can also be used.

## RESULTS AND DISCUSSION

The $\phi$ - $P$ (porosity vs. pressure) and $k$ – $P$ (permeability vs. pressure) behavior of the samples are very similar because of good correlation between porosity and permeability. We find distinctly different porosity-, and permeability- versus pressure dependencies for sandstones (Figures 2 and 3), and for limestones (Figures 3 and 4). The $\phi$ - $P$ and $k$ – $P$ curves for sandstone samples are convex from upwards, and can be expressed analytically as:

$$\phi(P) = \phi_1 + \phi_2 \, exp(-\alpha P), \tag{1}$$

$$k(P) = k_1 + k_2 \, exp(-\beta P), \tag{2}$$

where $\phi(P)$ and $k(P)$ are the porosity and the permeability, respectively, at a given confining pressure $P$, $\phi_1$ and $k_1$ are minimum porosity and permeability values at confining pressure approaching infinity. The constants $\phi_2$ and $k_2$ and the exponents $\alpha$ and $\beta$ are obtained by nonlinear least squares data fitting by the Gauss-Newton algorithm with Levenberg-Marquardt modifications for global convergence. This is implemented in MATLAB using the NLINFIT subroutine. The range of $r^2$-coefficients obtained for the least squares data fitting is given in Table 1. It is found that the exponents are in the range $0.008 < \alpha < 0.042$ and $0.01 < \beta < 0.14$ for the sandstone samples. All these samples are classified as quartzwacke with compressible pores. The porosity and permeability at zero confining pressure can be calculated as:

$$\phi(0) = \phi_1 + \phi_2 , \; k(0) = k_1 + k_2 \; . \qquad (3, 4)$$

Similarly, the porosity and permeability at infinite confining pressure can be calculated as:

$$\phi(\infty) = \phi_1, \; k(\infty) = k_1. \qquad (5, 6)$$

Majority of the limestone samples have $\phi$ - $P$ and $k$ – $P$ curves convex from downwards. Analytically Equations (1) and (2) can describe this behavior too, but the only difference is that the constants $\phi_2$ and $k_2$ and the exponents $\alpha$ and $\beta$ will be negative. The porosity and permeability at zero confining pressure for limestone samples belonging to this group can be calculated using Equations (3) and (4). However, it is obvious that Equations (1) and (2), with negative $\phi_2$, $k_2$, $\alpha$ and $\beta$, do not have a limiting value at confining pressure approaching to infinity. It can be argued that this behavior of the limestone samples is transitory and that at higher confining pressures the grains in the limestone samples would rearrange to give a behavior similar to the one observed in sandstone samples at high confining pressure. The pores are predominantly incompressible in the range of 0 – 70 MPa. Hence it is observed that there is very little decrease in porosity and permeability till about 70 MPa. However, at higher pressures (> 70 MPa) there is a sharp decrease indicating pressures in excess of the yield point of the rock. A possible pore collapse of some brittle pores would have occurred. These samples are characterized by high porosity and permeability (> 100 md). Many of them are identified as grainstones in the range of 500 md.

The remaining limestone samples have a convex from upwards behavior both for the $\phi$ - $P$ and $k$ – $P$ curves and are characterized by small values of porosity and permeability. They are predominantly packstones with a combination of compressible and incompressible pores.

For some samples the $\phi$ - $P$ (and $k$ – $P$) curves are irregular. For sandstones this occurs in the presence of fractures or if the pores are clogged by clay; in limestones the coexistence of different types of porosities (intergranular, intragranular, vugular) might result in an irregular $\phi$ - $P$ relation. The porosity-permeability plot showed a power-law

relationship for all samples. The exponent in the $k \sim \phi^n$ law was found smoothly changing with pressure, and has a possible connection with the *fractal dimension D* of the rock's pore space (Korvin et. al.).

In Figure 6, the porosities obtained from Equation (3) are plotted against permeabilities from Equation (4). At zero confining pressure, the permeability increases with porosity. In Figure 7, the permeability exponent $\beta$ (see Equation (2)) is plotted against porosity at zero confining pressure. It is observed that exponent $\beta$ decreases with increasing porosity both for sandstone and limestone samples. In Figure 8, the porosity exponent $\alpha$ (see Equation (1)) is plotted against permeability at zero confining pressure. It is seen that exponent $\alpha$ decreases with increasing permeability. The correlation between $\alpha$ and $k$ is not as good as that observed between $\beta$ and $\phi$.

The ratio of permeability decline with increasing confining pressure is known to be highly variable (Jones, 1988; Jones and Owens, 1980; Wei et al., 1986). Permeability values at initial ($k_i$) and final ($k_f$) conditions are incorporated into a term that describes the amount of permeability retained ($k_d$):

$$k_d = k_f / k_i \tag{7}$$

Similarly the amount of porosity retained ($\phi_d$) can be defined as:

$$\phi_d = \phi_f / \phi_i \tag{8}$$

where $\phi_f$ is the final and $\phi_i$ is the initial porosity.

Figure 9 shows porosity retained at 82 MPa versus initial porosity at 4.12 MPa for sandstone and limestone samples. A general trend of higher retained porosity for more porous samples is evident from the figure for sandstone samples. Figure 10 shows permeability retained at 82 MPa versus initial permeability at 4.12 MPa for sandstone samples. As observed for porosity, the less the permeability of the sample the higher the permeability loss (Davies and Holditch, 1998; Davies and Davies, 1999). Three distinct groups of sandstone samples can be identified from figure 10. The samples having initial permeability < 0.1 md have the maximum loss of permeability. They have minimum retained permeability of about 0.1, implying a loss of 90 to 99.9% permeability during the uploading pressure cycle. These samples are grouped as those belonging to Rock Type I. In the second distinct group of sandstone samples (Rock Type II) with the initial permeability ranging from 0.1 to 10 md, the retained permeability varies between 0.1 and 0.5 indicating a permeability loss of 50 to 90%. The third group of sandstone samples (Rock Type III) have higher initial permeabilities (> 10 md). These samples undergo a minimum loss of permeability (~ 30 %) for the given pressure range. In the literature (Davies and Davies, 1999) these different rock types are shown to have different pore geometries.

Figure 9 also shows retained porosity versus initial porosity at 4.12 MPa for limestone samples. It is observed that the trend is different from the case of sandstones. There is a critical porosity (~ 15 %) which divides the limestone samples into two groups, each having distinct behavior. Samples having initial porosities less than critical porosity show that the lesser the initial porosity, the larger the porosity loss, whereas samples having initial porosities larger than critical porosity behave in the opposite way, i.e., the larger the initial porosity, the larger the porosity loss. Figure 10 shows retained permeability at 82 MPa versus initial permeability at 4.12 MPa for the same limestone samples. The presence of a critical permeability value is observed in this figure also. Samples having initial permeability less than the critical permeability have almost constant loss of permeability (~ 15 – 25 %). Samples having larger than critical permeability are divided into two distinct clusters as shown in Figure 10. Cluster I has retained permeability in the range of 0.5 – 0.75 and for cluster II the range is 0.05 and 0.3. Cluster I comprises of packstones with predominantly compressible pores. Cluster II which has very high permeability samples (some ~ 500 md) comprises of grainstones with predominantly incompressible pores. If the pores are incompressible it is expected that a greater portion of the initial permeability would be retained, but this cluster shows very low values of permeability retained. It is possible that some pores have collapsed in these rocks resulting in a permeability loss much greater than that of cluster I.

## CONCLUSIONS

Stress-dependent porosity and permeability behavior of a suite of Saudi Arabian reservoir core samples were studied. Half of the core samples were sandstones and the other half limestones. In general the porosity and the permeability decreased exponentially with an increase in confining pressure. Simple analytical expressions for this behavior have been found using nonlinear least square regression fit. For majority of the limestone samples the stress-dependent behavior is different from that of the sandstones. The analytical expressions used to model this behavior are similar in form to the ones used for sandstones but with opposite signs. The coefficients of porosity and permeability expressions found using nonlinear least square regression fit show good correlation. It is observed that the exponents $\alpha$ and $\beta$ decrease with permeability and porosity, respectively.

For sandstone samples the maximum loss of permeability and porosity occurs for samples with the least amount of initial permeability and porosity, respectively. An interesting fact was noticed in the case of limestone samples. The retained porosity increased, i.e., the loss of porosity decreased with increase in initial porosity up to a critical initial porosity, after which the loss of porosity increased with initial porosity. Limestone samples with initial permeabilities less than critical exhibited almost similar loss of permeability. Limestone samples having greater than critical permeability could be divided into two distinct groups. In the second group where the retained permeability is very low, possible pore collapse is expected. Hence the retained permeability versus initial permeability plot could indicate the presence of pore collapse in core samples.

**Acknowledgment**

The authors appreciate the support provided by the Research Institute and Earth Sciences Department at King Fahd University of Petroleum & Minerals, Dhahran, Saudi Arabia during this research. Some of the work presented in this paper is part of a study supported by Saudi Aramco.

## REFERENCES

Abdulraheem, A., Mohiuddin, M. A., Korvin, G., Awal, M. R., Khan, K., Khan, M. S., and Al-Ghamdi, A., "Parametric study of ultrasonic velocity using reservoir cores for enhancing seismic signatures for improved reservoir definition", *1999 SPE Technical Symposium*, Dhahran, Saudi Arabia, 1999, pp. 111-120.

Davies, J. P., and Holditch, S. A., "Stress-dependent permeability in low permeability Gas reservoirs: Travis peak formation, East Texas," *1998 SPE Rocky Mountain Regional Low-Permeability Reservoirs Symposium and Exhibition*, 1998, pp. 117-128.

Davies, J. P., and Davies, D. K., "Stress-dependent permeability: Characterization and modeling," *1999 SPE Annual Technical Conference and Exhibition*, 1999, pp. 1-15.

Hsieh, P. A., Tracy, J. V., Neuzil, C. E., Bredehoeft, J. D., and Silliman, S. E., "A Transient Laboratory Method for Determining the Hydraulic Properties of Tight Rocks-I. Theory," *Int. Journal of Rock Mechanics, Mineral Sciences & Geomechanical Astracts*, 1980, pp. 245-252.

Jones, F. O., and Owens, W. W., "A laboratory study of low-permeability gas sands," *JPT*, September 1980, pp. 1631.

Jones, S. C., "Two-point determination of permeability and pv vs. net confining stress," *SPE Formation Evaluation*, March 1988, pp. 235-241.

Jones, S. C., "A Technique for faster Pulse-Decay Permeability Measurement in Tight Rocks," SPE# 28450, 1994, pp. 907-914.

Korvin, G., Mohiuddin, M. A., and Abdulraheem, A., "Experimental investigation of the fractal dimension of the pore surface of sedimentary rocks under pressure", submitted to *Journal of Geophysical Research*.

Luffel, D. L., Howard, W. E., and Hunt, E. R., "Travis peak core permeability and porosity relationships at reservoir stress," *SPE Formation Evaluation*, September 1991, pp. 310-318.

McKee, C. R., Bumb, A. C., and Koenig, R. A., "Stress-dependent permeability and porosity of coal and other geologic formations," *SPE Formation Evaluation*, March 1988, pp. 81-91.

Tiab, D., and Donaldson, E., *Petrophysics: Theory and Practice of Measuring Reservoir Rock and Fluid Transport Properties*, Gulf Publishing, Texas, USA, 1996.

Wei, K. K., Morrow, N. R., and Brower, K. R., "Effect of fluid, confining pressure and temperature on absolute permeabilities of low-permeability sandstones," *SPEFE*, August 1986, pp. 413.

## NOMENCLATURE

| | |
|---|---|
| $P$ | Hydrostatic Confining Pressure |
| $\phi$ | Porosity |
| $\phi_i$ | Initial Porosity |
| $\phi_f$ | Final Porosity |
| $\phi_d$ | Porosity Retained (fraction) |
| $\phi_1$ | Minimum Porosity at very high Confining Pressure |
| $k$ | Permeability |
| $k_i$ | Initial Permeability |
| $k_f$ | Final Permeability |
| $k_d$ | Permeability Retained (fraction) |
| $k_1$ | Minimum Permeability at very high Confining Pressure |
| $\alpha$ | Porosity Exponent |
| $\beta$ | Permeability Exponent |

**Table 1:** The range of $r^2$ coefficients for least squares data fitting of Equations 1 and 2 for the sandstone and limestone samples.

| Lithology | $r^2$-coefficient | | | |
|---|---|---|---|---|
| | Porosity (Equation 1) | | Permeability (Equation 2) | |
| | Minimum | Maximum | Minimum | Maximum |
| Sandstone | 0.9291 | 0.9992 | 0.9827 | 0.9995 |
| Limestone | 0.9060 | 0.9981 | 0.8727 | 0.9977 |

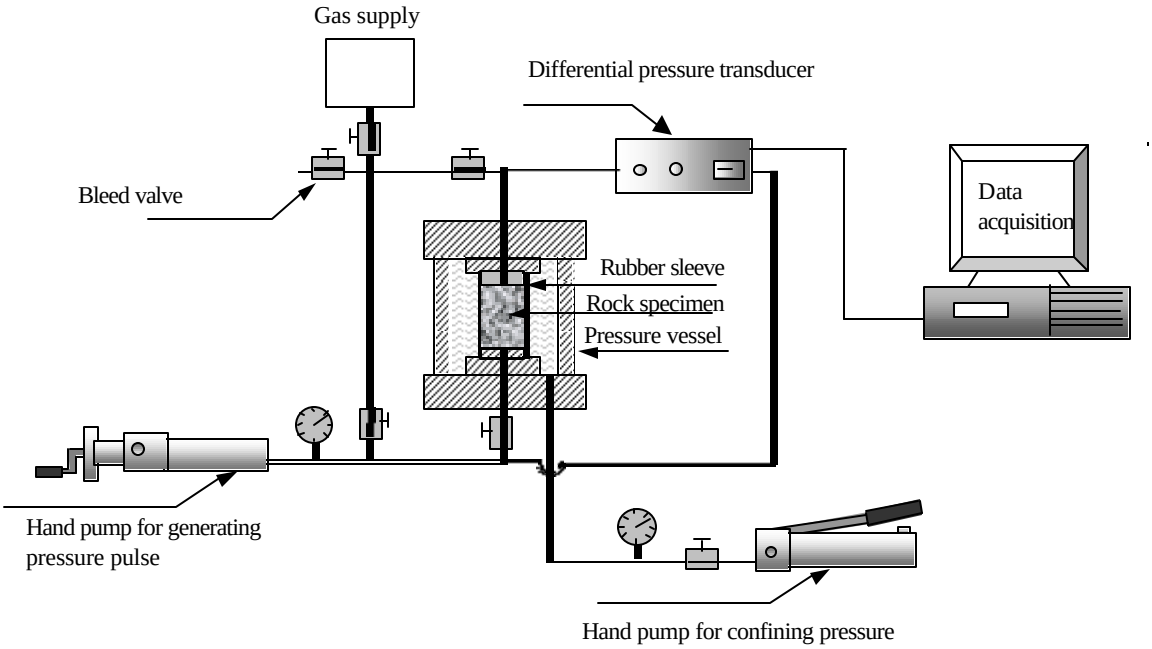


**Figure 1:** Schematic of the pressure pulse decay method for measuring permeability.

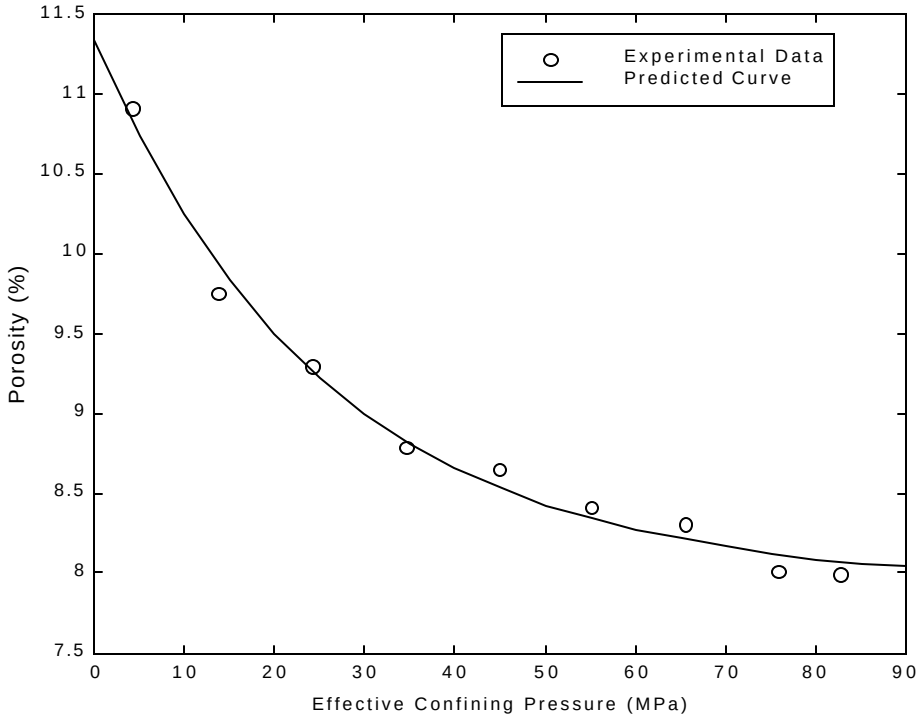


**Figure 2:** Porosity versus effective confining pressure curve with curve fit for a representative reservoir sandstone sample.

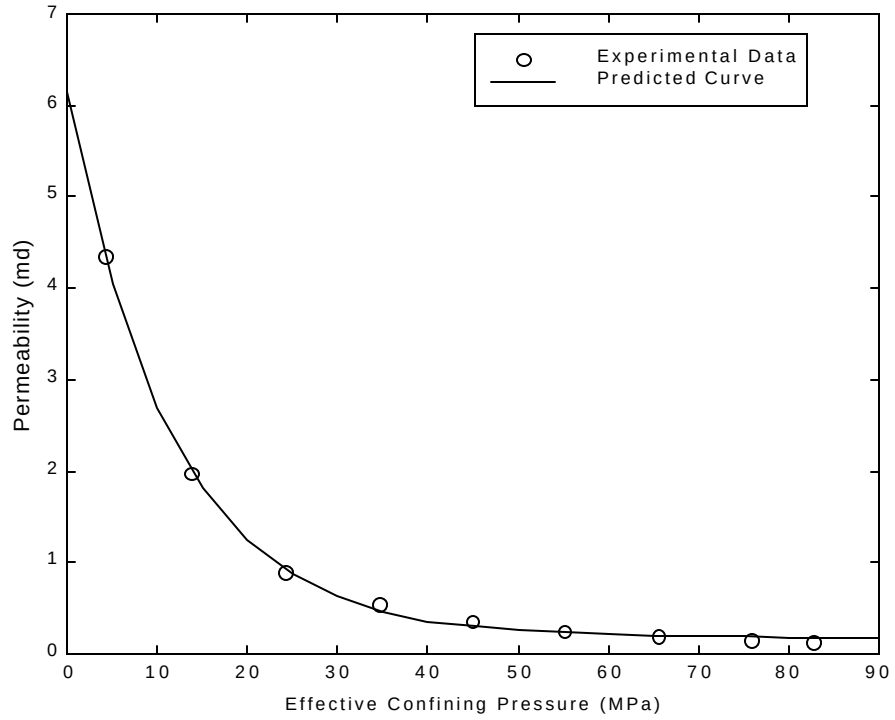


**Figure 3:** Permeability versus effective confining pressure curve with curve fit for a representative reservoir sandstone sample.

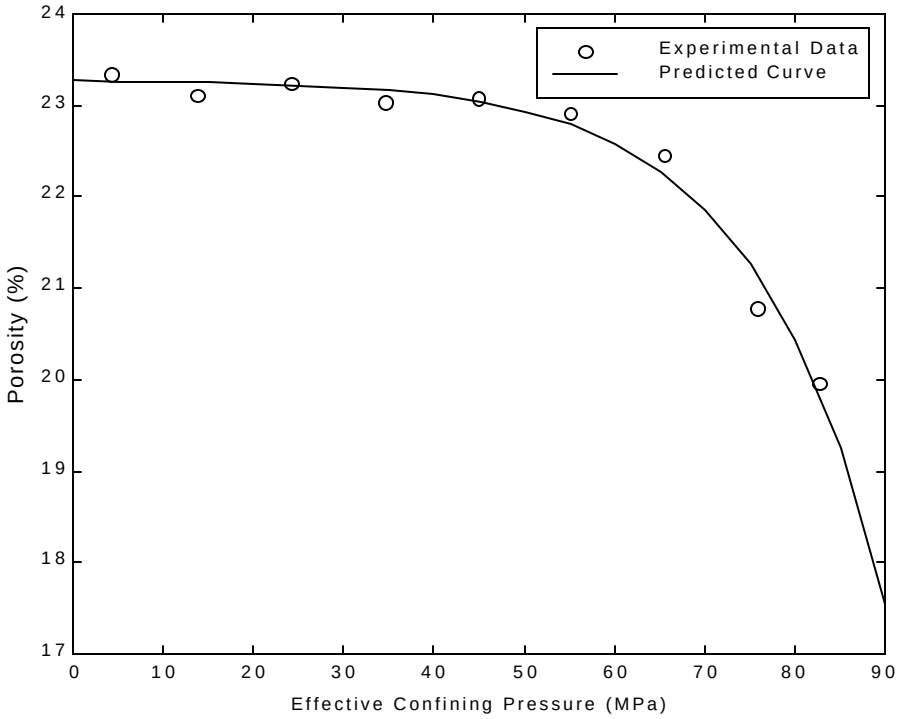


**Figure 4:** Porosity versus effective confining pressure curve with curve fit for a representative reservoir limestone sample.

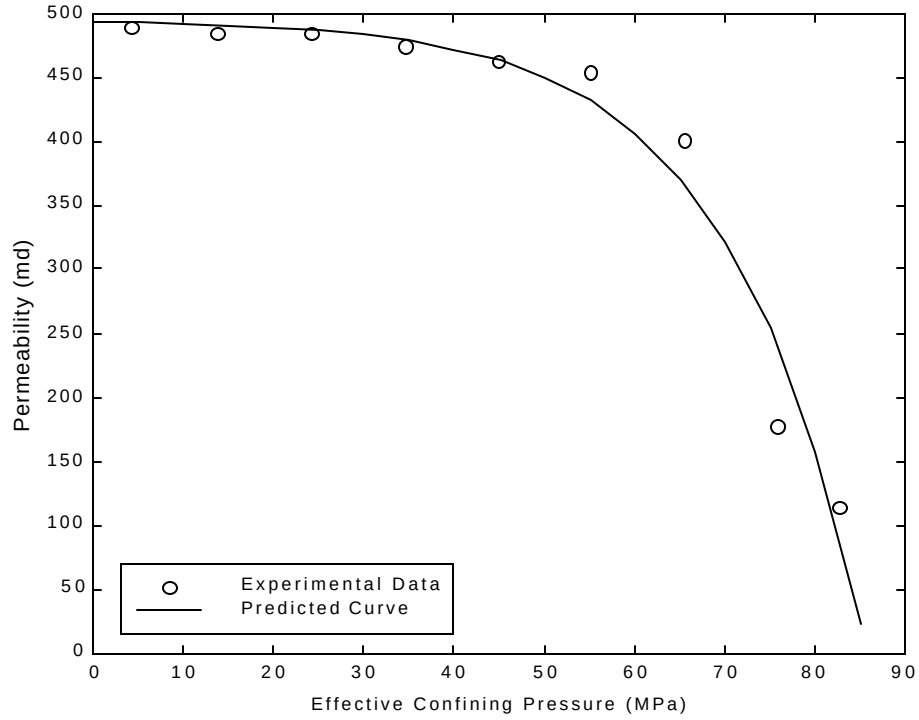


**Figure 5:** Permeability versus effective confining pressure curve with curve fit for a representative reservoir limestone sample.

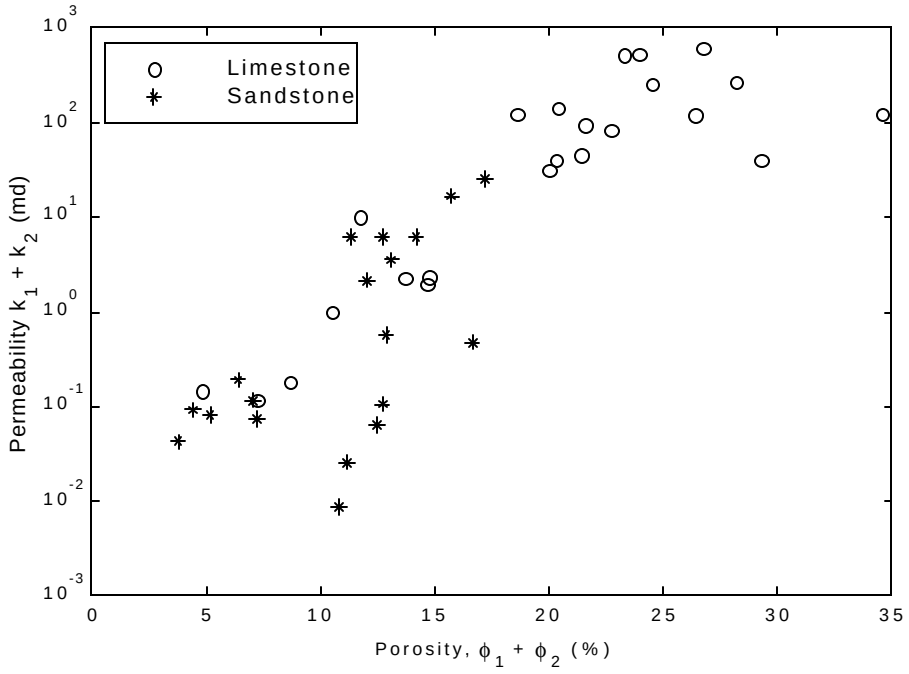


**Figure 6:** Regression-derived permeability vs. regression derived porosity at zero effective confining pressure.

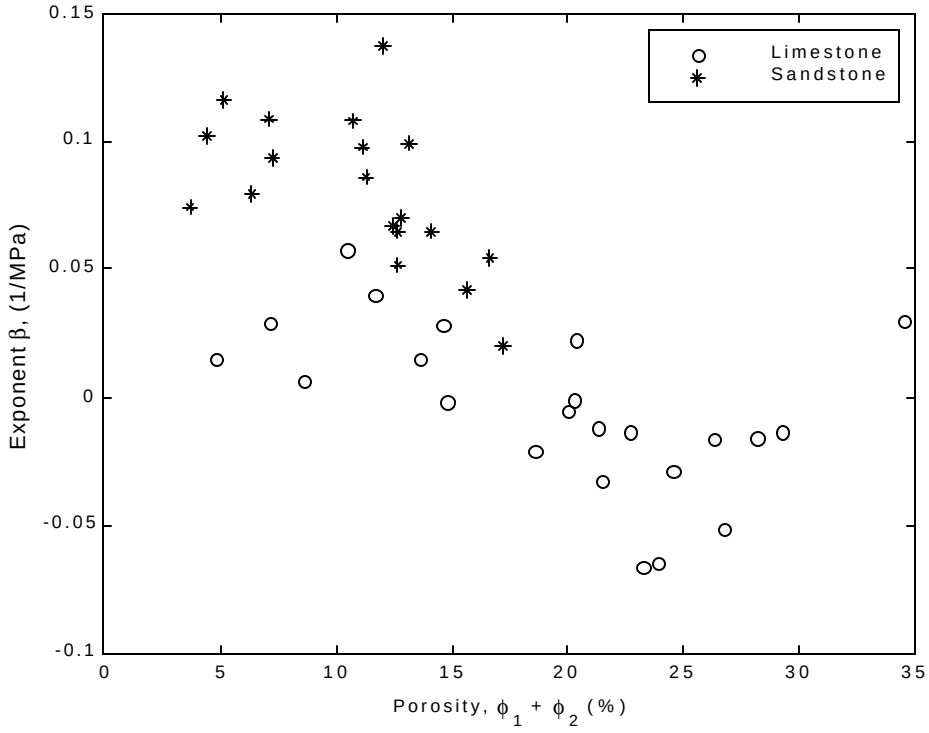


**Figure 7:** Porosity at zero effective confining pressure versus exponent β from the regression fits.

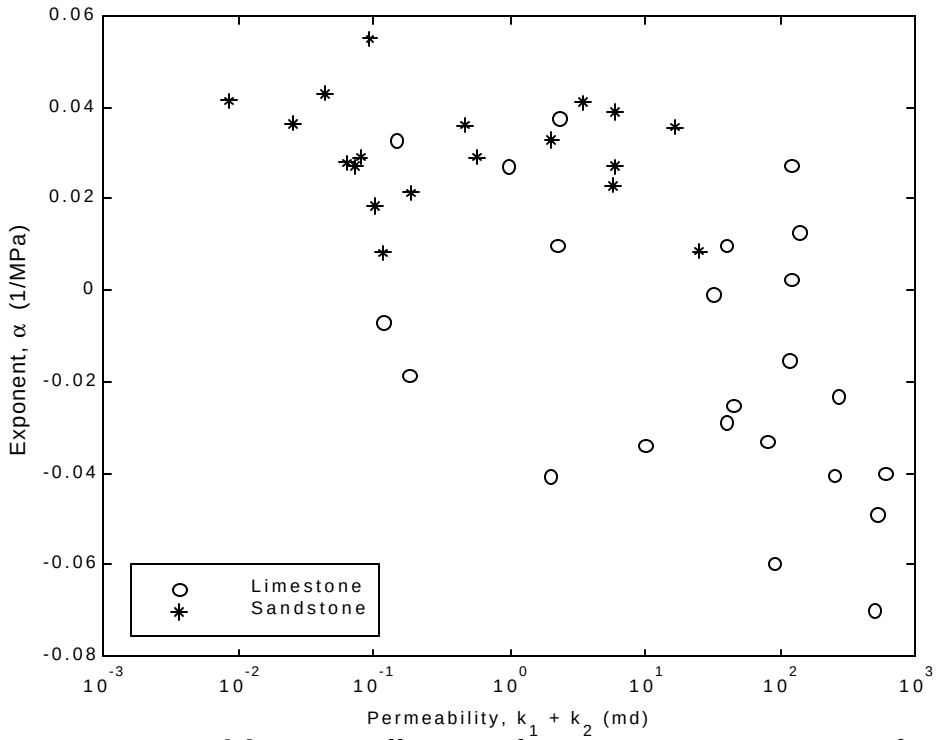


**Figure 8:** Permeability at zero effective confining pressure versus exponent α from the regression fits.

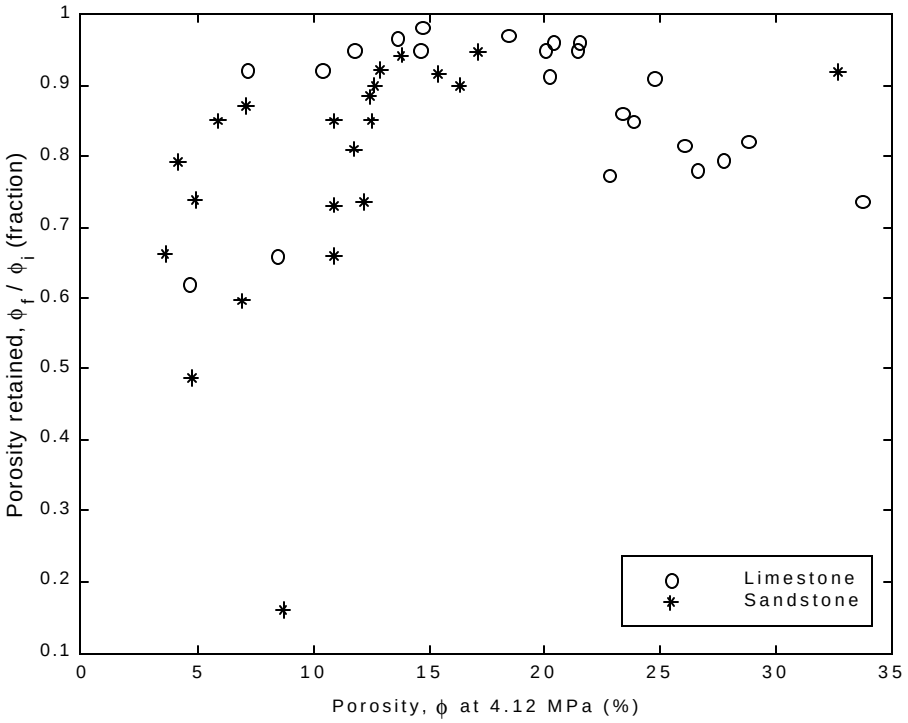


**Figure 9:** Porosity retained versus laboratory determined porosity at an effective confining pressure of 4.12 MPa.

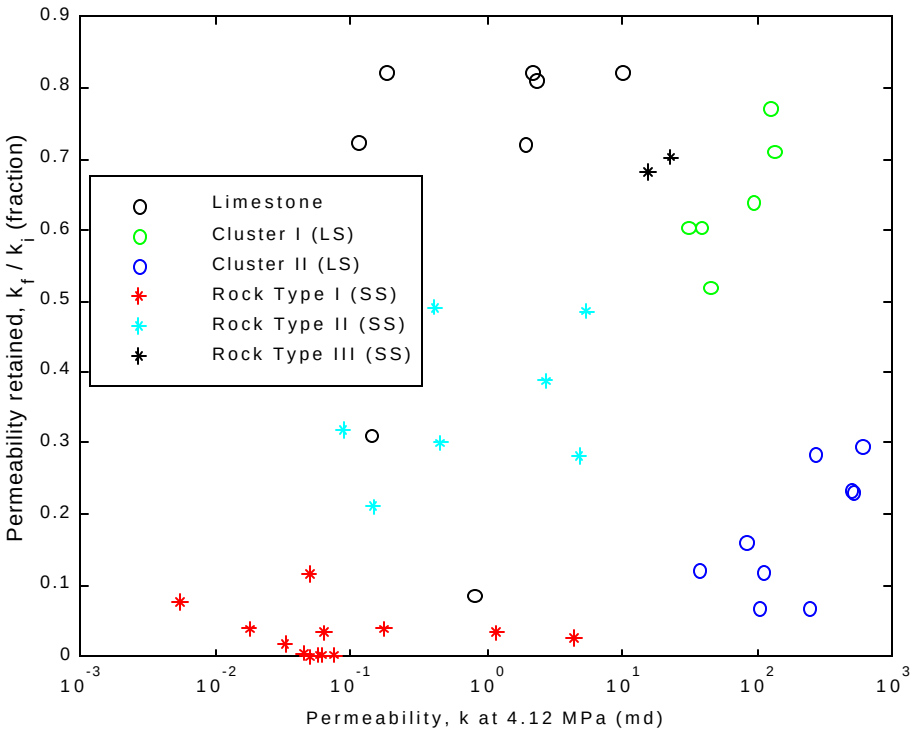


**Figure 10:** Permeability retained versus laboratory determined permeability at an effective confining pressure of 4.12 MPa.